Chemical Papers (2021) 75:2617–2624
https://doi.org/10.1007/s11696-021-01512-2

ORIGINAL PAPER

Synthesis of CoOx from ethaline on a stainless steel mesh for supercapacitor applications

Perihan Yilmaz Erdogan[1] · Abdulcabbar Yavuz[2] · Naime Ozdemir[1] · Huseyin Zengin[1]

Received: 15 September 2020 / Accepted: 12 January 2021 / Published online: 24 January 2021

Abstract

Room Temperature Ionic liquids (RTIL) are molten salts that are liquid at around room temperature and consist of asymmetric anions and cations. Low volatility and wide electrochemical potential behaviour of RTIL make them preferable in reaction synthesis and electrochemical applications. In this study, cobalt was electrochemically deposited on an inexpensive stainless steel mesh substrate. The resultant modified electrode was studied for supercapacitor applications by measuring its capacitance performance. Choline chloride and ethylene glycol-based ionic liquid called Ethaline was used as the deposition electrolyte, and the ionic liquid was contained a cobalt salt ($CoCl_2$) for cobalt growth. The deposition conditions of cobalt in Ethaline ionic liquid were found by cyclic voltammogram study. The cobalt in an ionic liquid was obtained by applying − 1.50 V potential on the stainless steel mesh by potentiostatic method. The uncoated and cobalt-coated steel mesh electrodes were then tested in KOH electrolyte to find appropriate potential window of the modified electrode. The cobalt-based material coated mesh electrode was scanned in 1 M KOH electrolyte between − 0.20 and 0.60 V and reported to have high electrochemical activity than uncoated mesh. The surface morphology of coated and uncoated mesh electrode was examined. Electrochemical characterizations of modified mesh electrodes were investigated using cyclic voltammetry. As a result, the obtained cobalt-coated mesh electrode had an areal capacitance of 650 mF cm^{-2} at scan rate of 5 mV s^{-1}. The cobalt-coated steel mesh electrode may have potential application in OH^--based electrolyte for energy storage devices.

Keywords Electrodeposition · Supercapacitor · Ionic liquid · Stainless steel mesh

Introduction

The use of portable devices, such as computers, medical devices and mobile phones, has recently increased widely with the rapid development of technology. It is important to store high amount of energy in these devices for later use. Batteries have been commonly used as energy storage systems in technological devices. High-performance supercapacitors have been studied as potential energy storage systems for such devices (Guerrero et al. 2009). Supercapacitors are divided into three groups as electrochemical double layer capacitors (EDLC), hybrid supercapacitors and pseudocapacitors (Hiralal et al. 2011). Supercapacitors have much higher capacitance (around 100 F g^{-1}) values than conventional capacitors. Therefore, it stores more energy than conventional capacitors (around few mF g^{-1}) (Shukla et al. 2000). Supercapacitors have high energy efficiency, long life and high power densities than batteries. Supercapacitors consist of two electrodes that allow energy storage by diffusion of ions and an ion-permeable separator between electrodes to prevent short-circuit electrical contact. The electrochemical property of the supercapacitors depends mainly on the materials used as the electrode and electrolyte. It depends significantly on the surface area of the electrode material, the wettability of the electrode, electrical conductivity of the components (electrode–electrolyte) and reaction between the electrode and electrolyte. Therefore, the selected electrode material is an important parameter for supercapacitor devices. It is important to develop electrodes with active and high surface area and to investigate the charge storage mechanisms at the electrochemical interface.

Metal oxides/hydroxide/sulphides [such as oxides/hydroxides/sulphides forms of nickel (Yavuz et al. 2019),

✉ Perihan Yilmaz Erdogan
yilmazperihan8@gmail.com

[1] Department of Chemistry, Gaziantep University, 27310 Gaziantep, Turkey

[2] Department of Metallurgical and Materials Engineering, Gaziantep University, 27310 Gaziantep, Turkey

cobalt (Godillot et al. 2011), vanadium (Boukhalfa et al. 2012), tin (Kuo et al. 2003), manganese (Wei et al. 2011)], conductive polymers [such as polypyrole (Zhang et al. 2019) and polyaniline (Zhang et al. 2010), polythiophene and their derivatives (Abas et al., 2019)] have been investigated for pseudocapacitor production. Carbon-derived materials and their composites have been prepared as electrode materials for EDLC devices (Boota et al. 2015). Aqueous solutions (acidic, alkaline or neutral) (Simon and Gogotsi 2010), organic solvents (Li et al. 2007) and ionic liquids may be used as electrolytes in supercapacitors. Room temperature ionic liquids have recently been studied for use as electrolytes in supercapacitors because of their electrical conductivities, electrochemical stabilities and wide potential windows (Zein El Abedin and Endres 2007). The operating conditions of the ionic liquids can typically be wide, for example, between − 35 and 250 °C because they generally have low vapour pressure (Dharaskarz 2012). Electrochemical stability is a measure of the oxidation and reduction in the electrode in the electrolyte solution. In principle, electrolytes with a large potential window may cause higher specific energy in supercapacitors. Unlike conventional solvents, ionic liquids consist of only ions and have high thermal stabilities, high ionic conductivities and chemical stabilities. Therefore, ionic liquids are of great interest for supercapacitor applications. In addition, ionic liquids could be used as an effective inhibitor solvent to prevent corrosion of materials such as copper (Vastag et al. 2018). Considering the studies conducted by various researchers, it was observed that metals with their oxides/hydroxide forms could be obtained in ionic liquids as energy storage devices (Liu et al. 2019a, b). Ionic liquids could also be used as an electrolyte in energy storage devices because redox reactions of electrolyte may contribute positively to the capacitance value (Wang et al. 2015).

Numerous coating methods, including physical vapour deposition (Smolin et al., 2017), chemical vapour deposition (Lobiak et al. 2017), sol–gel, diffusion coating (Chen and Xue 2016), hot-dip and several powder formation techniques, such as, hydrothermal (solvothermal) (Vattikuti et al. 2018), atomization and chemical reduction, have been investigated in order to obtain electroactive materials for energy storage devices. Besides these techniques, electrodeposition can also be applied for modification of the electrode because electrodeposition is easy to apply, inexpensive and materials surface could be controlled by altering growth conditions (pH, temperature, composition of the electrolyte) (Chen et al. 2015). Electrochemical reactions take place at the electrode and solution interfaces by the transfer of electrons. Since reactions take place at the interface, the conditions are quite favourable and have high selectivity. They generally do not create materials having contaminations after the growth reactions. Safavi et al. (2011) and Zhao et al. (2011) obtained electrodes electrochemically by coating the stainless steel mesh electrode for supercapacitors. In this study, the Co^{2+} contained Ethaline ionic liquid electrolyte was used for the electrodeposition of cobalt-based coating on a stainless steel mesh electrode. The aim of this study was to characterize the capacitance behaviour of cobalt coated steel mesh in alkaline solution.

Experimental section

Potassium hydroxide (KOH, Merck, 90%), ethylene glycol ($C_2H_6O_2$, Merck, 99%) (EG), cobalt (II) chloride ($CoCl_2{\cdot}6H_2O$, Merck, 98%), choline chloride ($HOC_2H_4N(CH3)_3Cl$, Merck, 98%) (ChCl) were used without further purification. The ionic liquid called Ethaline was prepared by stirring ChCl and EG (1:2 mol ratio) (see Fig. 1) at 55 °C until a transparent solution was obtained. $CoCl_2$ solution was then prepared with the resulting ionic liquid. Stainless steel mesh electrodes were just washed with deionised water. The electrochemical measurements in this study were conducted using a potentiostat with a three-electrode system. (VersaSTAT 3, Oak Ridge, the USA). Three-electrode cells including a stainless steel mesh working electrode, platinum wire secondary electrode were used. Ag/AgCl and Ag wire were the reference electrode used in aqueous solution and ionic liquid, respectively. Ag–AgCl containing 3 M KCl was used in aqueous solution, but was not used in the Ethaline electrolyte because water in the Ag–AgCl (3 M KCl) reference electrode may mix with the ionic liquid, and this could change the potential of measurements. The size of counter electrode was larger than the size of the working stainless steel mesh electrode to avoid limiting reaction of counter electrode as the focus is the reaction occurring on the working electrode. Stainless steel mesh electrode was immersed in the prepared Ethaline solution containing cobalt salt, and cobalt electrodeposition was performed by applying − 1.50 V potential. 1 M KOH electrolyte was used for electrochemical characterizations of the resulting electrode. Cyclic voltammograms were recorded at different scan rates, and their areal capacitance was calculated. All deposition experiments were performed at 55 °C, and electrode characterizations were conducted at room

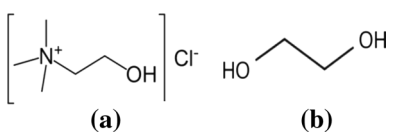

Fig. 1 Structure of **a** choline chloride and **b** ethylene glycol. Ethaline ionic liquid was obtained by mixing a part of choline chloride (ChCl) (panel **a**) and two part ethylene glycol (EG) (panel **b**)

temperature (22 ± 2 °C). Electrode surfaces were examined using an upright microscope (Nikon Eclipse LV15ONL) (Fig. 1).

Results and discussions

Deposition of CoOx on stainless steel mesh electrode

Before electrodeposition of cobalt potentiostatically, cyclic voltammetry of ionic liquid containing cobalt salt (Fig. 2a) was studied. Figure 2a shows the cyclic voltammetry curve of pure Ethaline solution (without $CoCl_2$) from − 2.0 to 1.0 V with the bare stainless steel mesh electrode. It appeared that the bare stainless steel mesh electrode was not electrochemically active in the Ethaline solution between − 1.0 and 0.20 V. Figure 2b illustrates the cyclic voltamogram of stainless steel mesh electrode in the ionic liquid media having $CoCl_2$ cycled from − 2.0 to 1.0 V at 50 mV s^{-1} scan rate. The cyclic voltammetry technique was conducted to determine the range of voltage at which electrodeposition and dissolution of cobalt were effective. Cyclic voltamogram was started from − 0.40 V in which there was no redox reaction of cobalt (open circuit potential) to − 2.0 V to observe whole reduction reaction of Co^{2+}. It was then cycled until + 1.0 V for dissolution of reduced cobalt. A reduction (in Fig. 2b) started at around − 1.0 V could be related to the reduction in Co^{2+} to metallic cobalt or hydrogen evolution (from H^+ to H_2). Abbott et al. (2006a) suggested that hydrogen evolution could occur at metal surfaces because of either hydrogen bond donor (ethylene glycol in Ethaline) (Alesary et al. 2019), or traces of water (Abbott et al. 2006a). Ionic liquids may absorb water at room conditions (Mele et al. 2003), and this trace of water may cause hydrogen evolution (Abbott et al. 2006b). To understand exact reaction (either hydrogen evolution or metal deposition) occurred in Ethaline, a cyclic voltamogram experiment without $CoCl_2$ was conducted and presented as Fig. 2a. A reduction was started at − 1.0 V when Ethaline did not have Co^{2+}. Therefore, the reduction started at − 1 V with $CoCl_2$ (Fig. 2b) could belong to hydrogen evolution. Reduction current of pure Ethaline solution was around 10 mA at − 1.20 V, but was five times greater when the Ethaline solution contained 200 mM $CoCl_2$ at − 1.20 V. This current difference must be related to cobalt deposition at the potential of − 1.20 V. Therefore, a voltage which is more negative than − 1.20 V can lead to cobalt deposition. Two reduction reactions (hydrogen evolution and electrodeposition of cobalt) could increase at more negative potential. Bubbles belonging to hydrogen gas were significantly more at − 1.50 V than at the potential of − 1.20 V. Cobalt film was obtained after long duration at − 1.20 V. Therefore, the potential of − 1.50 V was applied for the electrodeposition of cobalt at short durations (250 s).

It was aimed to obtain cobalt on stainless steel mesh in this study. Firstly, the stainless steel mesh electrode was immersed in choline chloride-ethylene glycol mixture containing 0.20 M $CoCl_2$ with − 1.50 V applied at room temperature. However, the cobalt coating seen by the naked eye was obtained after long duration of time, typically after around 1000 s. Therefore, the growth of the cobalt depending on temperature was studied by cyclic voltammetry. Cyclic voltamogram responses of stainless steel mesh in Ethaline ionic liquid containing $CoCl_2$ at 50 mV s^{-1} at two different temperature (room temperature and 55 °C) are presented in Fig. 3a. The current value of stainless steel mesh in Ethaline at room temperature and at 55 °C was approximately 5 mA and 50 mA at − 1.20 V. As charge (current multiplied by

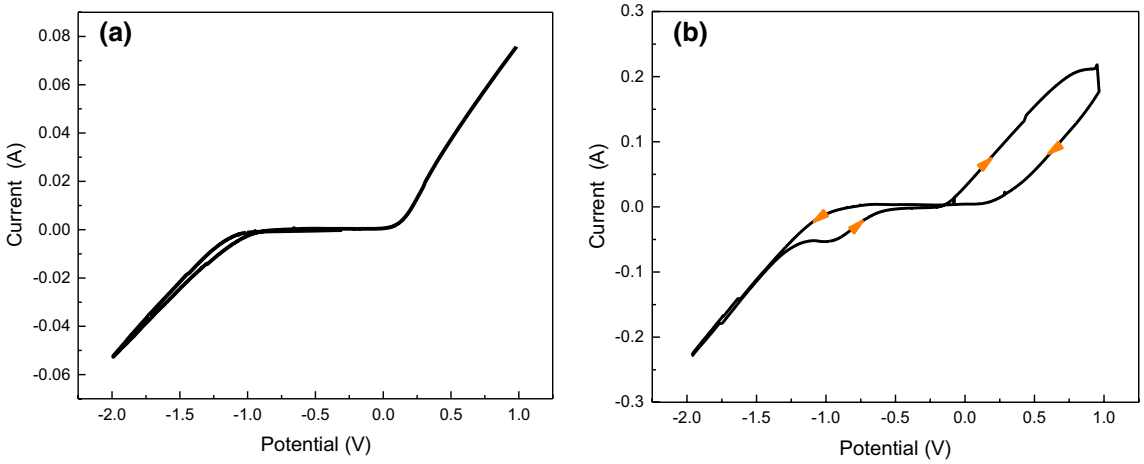

Fig. 2 **a** cyclic voltamogram curve of stainless steel mesh in a pure Ethaline (without $CoCl_2$) in a potential range of − 2 to 1 V at 55 °C. **b** cyclic voltamogram curve of Ethaline solution containing $CoCl_2$ and the working electrode was the stainless steel mesh. The scan rates of these experiments were 50 mV s^{-1}

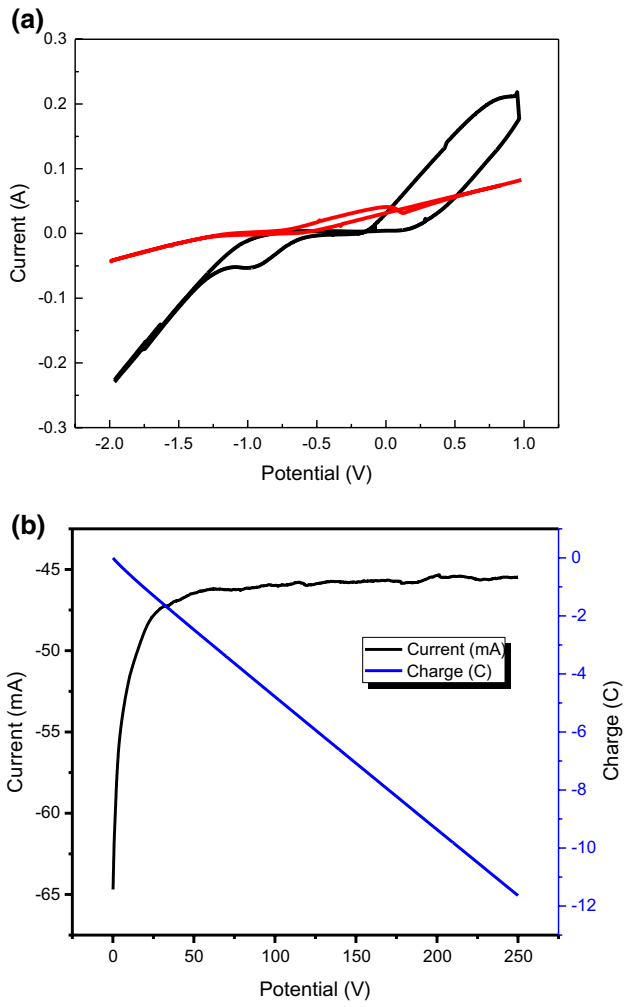

Fig. 3 **a** cyclic voltamogram curve of Ethaline solution containing $CoCl_2$ at room temperature (red line) and 55 °C (black line). The working electrode was the stainless steel mesh and the scan of the experiments was 50 mV s^{-1}. **b** Chronoamperometric (current vs. time) and chronocoulometric (charge vs. time) curve of the cobalt electrodeposition by applying − 1.5 V potential for 250 s on the stainless steel electrode in Ethaline medium containing Co^{2+}. The electrolyte temperature was 55 °C

time) of the electrodeposition was greater at high temperature, the electrolyte temperature of 55 °C may lead to greater cobalt deposition. Cobalt-based film was electrodeposited on stainless steel mesh electrode surface by chronoamperometric method. Figure 3b shows the chronoamperometric data obtained by the application of − 1.50 V when stainless steel mesh electrode was in cobalt-contained ionic liquid for 250 s at 55 °C. After obtaining cobalt-based film, it was scanned between − 0.20 and 0.60 V in KOH electrolyte to determine its electrochemical performance. A small fluctuation of current in the graph may be caused by hydrogen gas evolution. The charge during cobalt electrodeposition was 12 C because of cobalt electrodeposition and also hydrogen evolution. Electrodeposition of metals with hydrogen evolution was determined by EQCM measurement in the literature (Abbott et al. 2016).

Characterization of electrodes

Figure 4 illustrates both images of an uncoated and cobalt-coated steel mesh. The microscopic image of the uncoated steel mesh is presented in Fig. 4a. Figure 4a is an upright microscope view of the bare stainless steel mesh electrode. It was shiny metallic grey as it did not have coatings on its surface. This microscopic image was taken from uncoated part of steel mesh photographed in Fig. 4b (given as light-coloured part). Cobalt-coated part of steel by applying − 1.50 V for 250 s from Ethaline was greenish grey (see right hand side of Fig. 4b). The surface of cobalt coated part of steel mesh was examined under an optical microscope presented in Fig. 4c. It was observed that the network structures of the bare stainless steel mesh electrode were filled with electrodeposited cobalt. Cobalt was completely coated on the surface of mesh substrate.

Figure 5a illustrates the cyclic voltammetry curves of electrodes scanned in a 1 M KOH electrolyte to examine the electrochemical behaviour of a cobalt-based stainless steel mesh electrode (red line) and a bare stainless steel mesh electrode (black line). In Fig. 5a, no oxidation or reduction peaks were observed for the bare stainless steel mesh

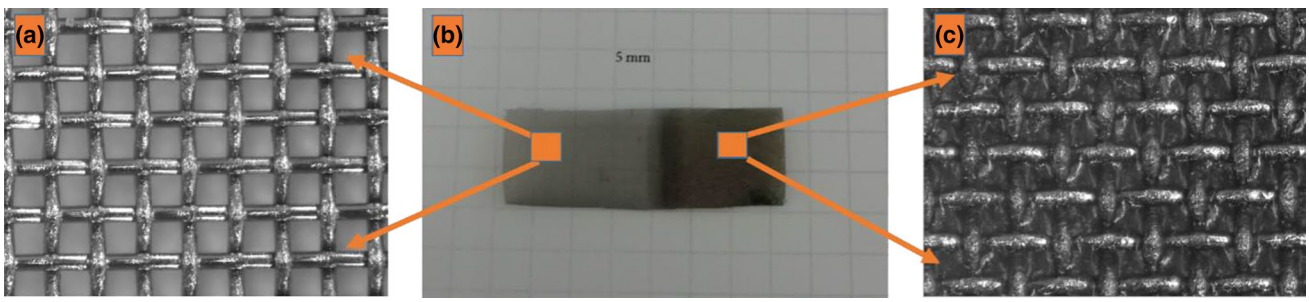

Fig. 4 Images of (**a**) bare stainless steel mesh electrode **b** non-cobalt-deposited (light-coloured part) and cobalt deposited (dark-coloured part) stainless steel mesh electrode **c** cobalt-deposited steel mesh electrode

electrode (black line) in 1 M KOH electrolyte. However, a pair of reversible redox peaks belonging to coated mesh were observed in KOH electrolyte. An oxidation at 0.20 V and the other one at 0.5 V were observed for the cobalt-based stainless steel mesh electrode (red line Fig. 5a). The reduction at 0.35 V was expected to be either a desorption of oxygen which adsorbed at around 0.60 V or the reduction in cobalt-based film. In order to analyse the reduction peak at around 0.35 V, the experiment was repeated by narrowing the range of potential. The potential range of modified electrode cycling in KOH was limited (from − 0.20 to 0.45 V) at different scan rates. The experiment is given as Fig. 5b. As there was still a reduction peak of cobalt-based film cycling in KOH at 50 mV s^{-1} (blue line of Fig. 5b) at around + 0.35 V, this peak belonged to the modified electrode. It was not related to oxygen adsorption reaction. The redox current of coated mesh was significantly increased compared to bare steel mesh electrode because the cobalt-based film deposited on the surface of the bare stainless steel mesh electrode had a great active surface area (Fig. 5a). The redox peaks in the alkaline solution of the cobalt coated mesh proves electroactivity of cobalt. Thus, when the cobalt-based steel mesh electrode was placed in the KOH solution and scanned between − 0.20 and 0.60 V as shown in Fig. 5a, the oxidation and reduction peaks of the cobalt became visible.

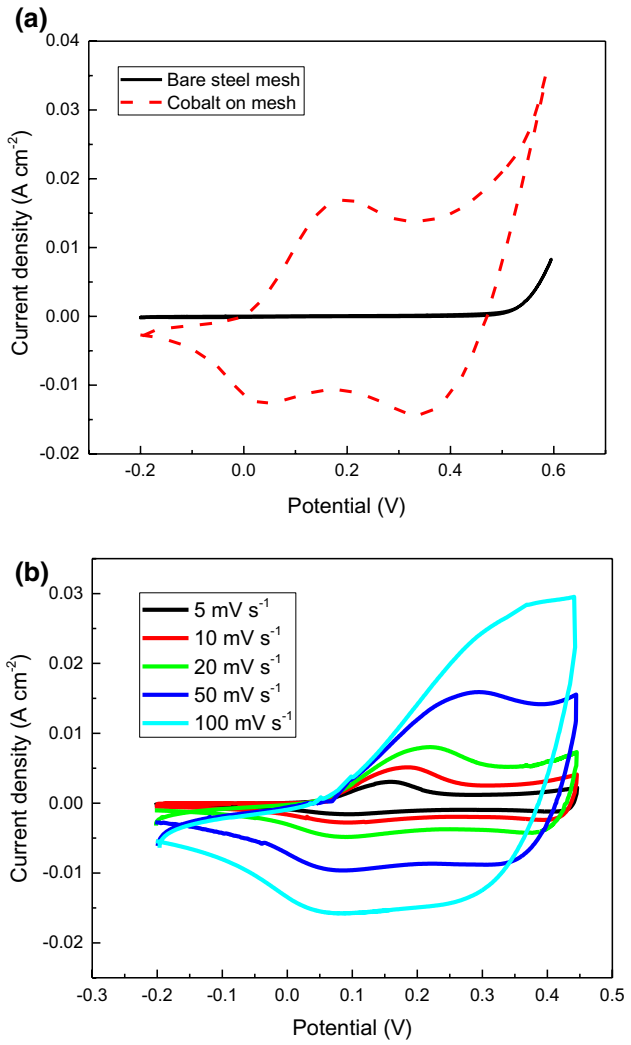

Fig. 5 **a** Cyclic voltammogram curve of bare steel mesh electrode (black solid line) and cobalt coated stainless steel mesh electrode (red dashed line) in KOH electrolyte at 50 mV s^{-1} scan rate. **b** Cyclic voltammogram curves of cobalt film electrodeposited on mesh cycling in 1 M KOH electrolyte at different scan rate (5, 10, 20, 50 and 100 mV s^{-1}) between − 0.20 and 0.45 V

The cyclic voltammograms of the cobalt-based stainless steel mesh in 1 M KOH at different scan rates were also investigated at the potential window between − 0.20 and 0.60 V and presented in Fig. 6. The redox current increases from 5 to 100 mV s^{-1} upon increasing scan rate which is related to improved ion transfer within the material within a short time. Wide oxidation and reduction peaks were obtained at the different scan rates. It was clear that the film deposited on the stainless steel surface and had a high areal capacity at all available scan rates. Areal capacitance of cobalt-based material on mesh depended on the scan rate and was calculated and presented in Fig. 7. The areal capacitance was calculated by using Eq. 1:

$$C_s = \frac{i \cdot t}{\Delta U \cdot S} \tag{1}$$

C_s areal capacitance, i current (A), t the time (s), ΔU the potential window (V), S the working area of electrode (cm^2). The decrease in capacitance with increasing scan rate is probably due to the rate of ion transfer at larger timescale

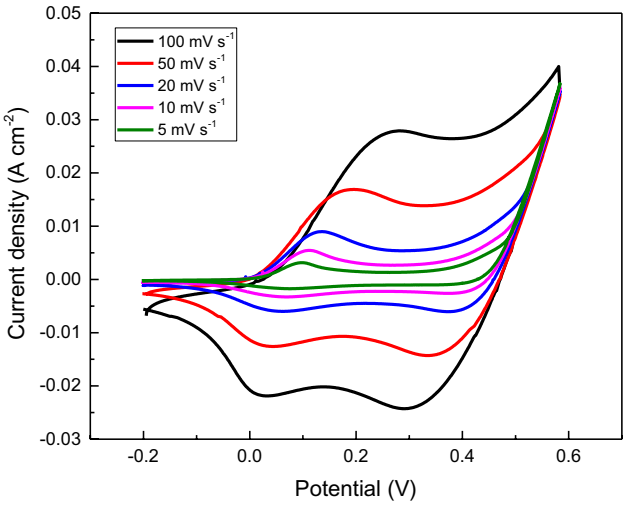

Fig. 6 Cyclic voltammogram curves of cobalt film electrodeposited on mesh cycling in 1 M KOH electrolyte at different scan rate (5, 10, 20, 50 and 100 mV s^{-1}) between − 0.20 and 0.60 V

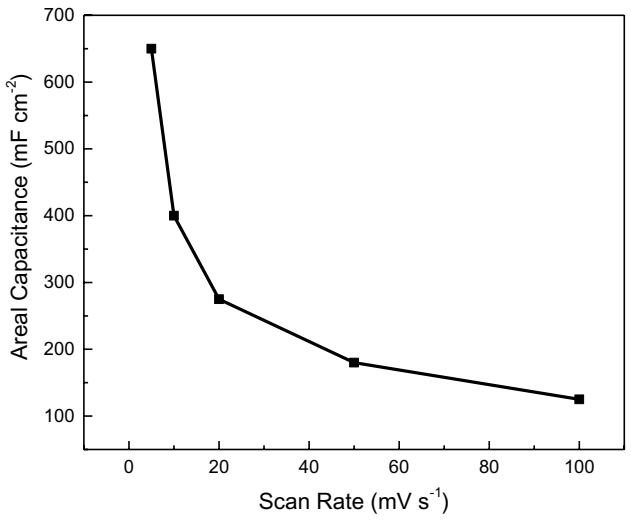

Fig. 7 Variations of areal capacitances of Co coated mesh in KOH at different scan rates. Data of Fig. 6 were used to calculate the areal capacitance

(Zhou et al. 2009). The areal capacitance was found to be 650 mF cm $^{-2}$ at a scan rate of 5 mV s^{-1} (see Fig. 7).

The mesh electrode consisted of grits including gaps between filaments and the real area, dependent on deposited cobalt or its active surface, was not calculated as this included the inner surface of the electrode. The area of the electrode (stainless steel mesh) used as the working electrode was calculated as the outer surface (geometric surface). The areal capacitance of the cobalt-based stainless steel mesh electrode was calculated based on cyclic voltammogram curves (Fig. 6) at various scan rate (5, 10, 20, 50 and 100 mV s^{-1}). As shown in Fig. 7, the areal capacitance decreases as the scan rate increases, and the areal capacitance at 5 mV s^{-1} was found to be 650 mF cm^{-2}. Areal capacitance of the modified electrode at 100 mV s^{-1} was found to be 125 mF cm^{-2}. The higher capacitance at the lower scan rate may be due to longer contact of the electrode in the electrolyte solution (Cai et al. 2011). Improvements in the capacitive properties of the cobalt film may be due to the electrodeposition of a uniform thin cobalt film on the wires of steel mesh surface which significantly increased the surface coverage of the electrode (Chodankar et al. 2017). The areal capacitance of cobalt-based electrode obtained from Ethaline ionic liquid was compared with the areal capacitance of electrodes obtained by different synthesis media and growth method in Table 1.

Conclusion

Ionic liquid electrolyte usage for the electrodeposition of cobalt for supercapacitor production was shown in this study. The cobalt salt contained ionic liquid was used as the deposition electrolyte to obtain cobalt coating on the stainless steel mesh by potentiostatic deposition. Cyclic voltammogram technique was used to examine growth conditions, such as deposition potential and electrolyte temperature, of cobalt in Ethaline ionic liquid. A potential which is more negative than − 1.2 V and high temperature lead to electrodepositions of cobalt. Cobalt deposition was obtained by the application of a constant potential of − 1.50 V, and resulting electrode was subsequently scanned between − 0.20 and 0.60 V in 1 M KOH electrolyte to determine its electrochemical activity. The cobalt-based steel mesh electrode provided improved electrochemical performance in alkaline media. The attainment of high surface area electrodes in supercapacitors may significantly affect capacitance. In this study, electrode material with high surface coverage was obtained by electrodeposition of cobalt film on steel mesh which had high surface areas, but stainless steel mesh was not electrochemically active in alkaline electrolyte. Therefore, the electrodeposited cobalt film on mesh may be used directly as an electrode in supercapacitor applications. The cobalt coated steel mesh electrode was found to have an areal capacitance of maximum 650 mF cm^{-2} at scan rate of 5 mV s^{-1} in the KOH electrolyte. The electrodeposition of cobalt on stainless steel mesh electrode in Ethaline ionic liquid media can

Table 1 Areal capacitance of modified electrodes reported in the literature

Synthesis media	Method	Capacitance	Electrode	References
Aqueous solution	Hydrothermal method	2.51 F/cm^2	Mn_3O_4-MnOOH	Meng et al. (2018)
Aqueous solution	In situ chemical bath method	58.5 mF/cm^2	$Ni_3V_2O_8$ and PANI electrode	(Liu et al. 2018)
Ethaline	Solvothermal	5.63 mF/cm^2	Ni_3S_2 on Ni foam	(Chen et al. 2020)
Aqueous solution	Chemical method	2.30 F/cm^2	$CuCo_2O_4$@NiO electrode	(Xu et al. 2019)
Ionic liquid	Chemical vapour deposition	0.29 mF/cm^2	Graphene electrodes	(Zang et al. 2014)
Ionic liquid	Wet-spinning method	597 mF/cm^2	MWCNTs-rGOs-cellulose fibres electrodes	(Liu et al. 2019a, b)
Aqueous solution	Chemical method	180 mF/cm^2	Graphene-stainless steel fabrics	(Yu et al. 2016)
Ethaline	Electrochemical method	650 mF/cm^2	CoOx/SS mesh	This study

be applied as an easy and cost-effective method to improve the capacitance performance of supercapacitors.

Acknowledgement Perihan Yilmaz Erdogan and Naime Ozdemir wish to thank YOK-Turkey for 100/2000 scholarship program.

References

Abas A, Sheng H, Ma Y, Zhang X, Wei Y, Su Q, Lan W, Xie E (2019) PEDOT: PSS coated CuO nanowire arrays grown on Cu foam for high-performance supercapacitor electrodes. J Mater Sci Mater Electron 30:10953–10960

Abbott AP, Alhaji AI, Ryder KS, Horne M, Rodopoulos T (2016) Electrodeposition of copper–tin alloys using deep eutectic solvents. Trans IMF 94(2):104–113

Abbott AP, Capper G, McKenzie KJ, Ryder KS (2006) Voltammetric and impedance studies of the electropolishing of type 316 stainless steel in a choline chloride based ionic liquid. Electrochim Acta 51(21):4420–4425

Abbott AP, McKenzie KJ (2006) Application of ionic liquids to the electrodeposition of metals. Phys Chem Chem Phys 8(37):4265–4279

Alesary HF, Cihangir S, Ballantyne AD, Harris RC, Weston DP, Abbott AP, Ryder KS (2019) Influence of additives on the electrodeposition of zinc from a deep eutectic solvent. Electrochim Acta 304:118–130

Boota M, Paranthaman MP, Naskar AK, Li Y, Akato K, Gogotsi Y (2015) Waste tire derived carbon-polymer composite paper as pseudocapacitive electrode with long cycle life. Chemsuschem 8(21):3576–3581. https://doi.org/10.1002/cssc.201500866

Boukhalfa S, Evanoff K, Yushin G (2012) Atomic layer deposition of vanadium oxide on carbon nanotubes for high-power supercapacitor electrodes. Energy Environ Sci 5(5):6872–6879

Cai YM, Qin ZY, Chen L (2011) Effect of electrolytes on electrochemical properties of graphene sheet covered with polypyrrole thin layer. Prog Nat Sci Mater Int 21(6):460–466. https://doi.org/10.1016/S1002-0071(12)60083-5

Chen H, Wei Z, Zheng X, Yang S (2015) A scalable electrodeposition route to the low-cost, versatile and controllable fabrication of perovskite solar cells. Nano Energy 15:216–226

Chen K, Xue D (2016) Colloidal supercapacitor electrode materials. Mater Res Bull 83:201–206

Chen L, Zeng J, Guo M, Xue R, Deng R, Zhang Q (2020) Deep eutectic solvent-assisted in-situ synthesis of nanosheet-packed Ni3S2 porous spheres on Ni foam for high performance supercapacitors. J Colloid Interface Sci 583:594–604

Chodankar NR, Dubal DP, Kwon Y, Kim DH (2017) Direct growth of $FeCo_2O_4$ nanowire arrays on flexible stainless steel mesh for high-performance asymmetric supercapacitor. NPG Asia Mater 9(8):e419. https://doi.org/10.1038/am.2017.145

Dharaskar SA (2012) Ionic liquids (a review): the green solvents for petroleum and hydrocarbon industries. Res J Chem Sci 2(8):80–85

Godillot G, Guerlou-Demourgues L, Taberna PL, Simon P, Delmas C (2011) Original conductive nano-Co_3O_4 investigated as electrode material for hybrid supercapacitors. Electrochem Solid-State Lett 14(10):A139. https://doi.org/10.1149/1.3609259

Guerrero MA, Romero E, Barrero F, Milanes MI, Gonzalez E (2009) Supercapacitors: alternative energy storage systems. Prz Elektrotech 85(10):188–195

Hiralal P, Wang H, Unalan HE, Liu Y, Rouvala M, Wei D, Andrew P, Amaratunga GAJ (2011) Enhanced supercapacitors from hierarchical carbon nanotube and nanohorn architectures. J Mater Chem 21(44):17810–17815

Kuo S, Wu N (2003) Composite supercapacitor containing tin oxide and electroplated ruthenium oxide. Electrochem Solid-State Lett 6(5):A85. https://doi.org/10.1149/1.1563872

Li W, Chen D, Li Z, Shi Y, Wan Y, Wang G, Jiang Z, Zhao D (2007) Nitrogen-containing carbon spheres with very large uniform mesopores: the superior electrode materials for EDLC in organic electrolyte. Carbon 45(9):1757–1763

Liu L, Wang X, Zhang X, Zhang X, Chen S (2019a) Ionic liquid electrodeposition of Ge nano-film on Cu wire mesh as stable anodes for lithium-ion batteries. Ionics 26:2225–2231

Liu X, Wang J, Yang G (2018) In situ growth of the Ni3V2O8@ PANI composite electrode for flexible and transparent symmetric supercapacitors. ACS Appl Mater Interfaces 10(24):20688–20695

Liu Y, Wang Y, Nie Y, Wang C, Ji X, Zhou L, Pan F, Zhang S (2019b) Preparation of MWCNTs-graphene-cellulose fiber with ionic liquids. ACS Sustain Chem Eng 7(24):20013–20021

Lobiak EV, Bulusheva LG, Fedorovskaya EO, Shubin YV, Plyusnin PE, Lonchambon P, Senkovskiy BV, Ismagilov ZR, Flahaut E, Okotrub AV (2017) One-step chemical vapor deposition synthesis and supercapacitor performance of nitrogen-doped porous carbon–carbon nanotube hybrids. Beilstein J Nanotechnol 8(1):2669–2679

Mele A, Tran CD, De Paoli Lacerda SH (2003) The structure of a room-temperature ionic liquid with and without trace amounts of water: the role of C-H···O and C-H···F interactions in 1-n-butyl-3-methylimidazolium tetrafluoroborate. Angew Chem 115(36):4500–4502

Meng S, Mo Z, Li Z, Guo R, Liu N (2019) Binder-free electrodes based on Mn_3O_4/γ-MnOOH composites on carbon cloth for supercapacitor application. J Solid State Chem 274:134–141

Nayak S, Soam A, Nanda J, Mahender C, Singh M, Mohapatra D, Kumar R (2018) Sol–gel synthesized BiFeO3–graphene nanocomposite as efficient electrode for supercapacitor application. J Mater Sci Mater Electron 29(11):9361–9368

Safavi A, Kazemi SH, Kazemi H (2011) Electrochemically deposited hybrid nickel-cobalt hexacyanoferrate nanostructures for electrochemical supercapacitors. Electrochim Acta 56(25):9191–9196. https://doi.org/10.1016/j.electacta.2011.07.122

Shukla AK, Sampath S, Vijayamohanan K (2000) Electrochemical supercapacitors: energy storage beyond batteries. Curr Sci 79(12):1656–1661

Simon P, Gogotsi Y (2010) Materials for electrochemical capacitors. Nanoscience and technology: a collection of reviews from nature journals. World Scientific, Singapore, pp 320–329

Smolin YY, Van Aken KL, Boota M, Soroush M, Gogotsi Y, Lau KKS (2017) Engineering ultrathin polyaniline in micro/mesoporous carbon supercapacitor electrodes using oxidative chemical vapor deposition. Adv Mater Interfaces 4(8):1601201

Vastag G, Shaban A, Vraneš M, Tot A, Belić S, Gadžurić S (2018) Influence of the N-3 alkyl chain length on improving inhibition properties of imidazolium-based ionic liquids on copper corrosion. J Mol Liq 264:526–533

Vattikuti SP, Nagajyothi PC, Anil Kumar Reddy P, Kotesh Kumar M, Shim J, Byon C (2018) Tiny MoO3 nanocrystals self-assembled on folded molybdenum disulfide nanosheets via a hydrothermal method for supercapacitor. Mater Res Lett 6(8):432–441

Wang Y, Guo J, Wang T, Shao J, Wang D, Yang YW (2015) Mesoporous transition metal oxides for supercapacitors. Nanomaterials 5(4):1667–1689. https://doi.org/10.3390/nano5041667

Wei W, Cui X, Chen W, Ivey DG (2011) Manganese oxide-based materials as electrochemical supercapacitor electrodes. Chem Soc Rev 40(3):1697–1721

Xu K, Ma S, Shen Y, Ren Q, Yang J, Chen X, Hu J (2019) CuCo2O4 nanowire arrays wrapped in metal oxide nanosheets as hierarchical multicomponent electrodes for supercapacitors. Chem Eng J 369:363–369

Yavuz A, Kaplan K, Bedir M (2019) Annealing of electrodeposited nickel on low carbon steel for supercapacitor applications. Dig J Nanomater Biostructures 14(4):1061–1068

Yu J, Wu J, Wang H, Zhou A, Huang C, Bai H, Li L (2016) Metallic fabrics as the current collector for high-performance graphene-based flexible solid-state supercapacitor. ACS Appl Mater Interfaces 8(7):4724–4729

Zang X, Li P, Chen Q, Wang K, Wei J, Wu D, Zhu H (2014) Evaluation of layer-by-layer graphene structures as supercapacitor electrode materials. J Appl Phys 115(2):24305

Zein El Abedin S, Endres F (2007) Ionic liquids: the link to high-temperature molten salts? Acc Chem Res 40(11):1106–1113

Zhang K, Zhang LL, Zhao XS, Wu J (2010) Graphene/polyaniline nanofiber composites as supercapacitor electrodes. Chem Mater 22(4):1392–1401

Zhang X, Gao M, Tong L, Cai K (2019) Polypyrrole/nylon membrane composite film for ultra-flexible all-solid supercapacitor. J Materiomics 6(2):339–347

Zhao T, Jiang H, Ma J (2011) Surfactant-assisted electrochemical deposition of α-cobalt hydroxide for supercapacitors. J Power Sources 196(2):860–864. https://doi.org/10.1016/j.jpowsour.2010.06.042

Zhou WJ, Xu MW, Zhao DD, Xu CL, Li HL (2009) Electrodeposition and characterization of ordered mesoporous cobalt hydroxide films on different substrates for supercapacitors. Micropor Mesopor Mat 117(1–2):55–60. https://doi.org/10.1016/j.micromeso.2008.06.004